Tuijin Jishu/Journal of Propulsion Technology
ISSN: 1001-4055
Vol. 46 No. 1 (2025)

A Wide Conversion Ratio Bidirectional Modified SEPIC Converter with Non Dissipative Current Snubber

Chitra L[a*] , Kothaiandal C[b] , Saravanakumar M[a], Manikandan K[a],

[a]Department of Electrical and Electronics Engineering, Dr. Mahalingam College of Engineering and Technology,

Pollachi, Tamilnadu, INDIA - 642003

[b]Department of Electrical and Electronics Engineering, AMC College of Engineering,

Bengaluru, Karnataka, India -560083

Abstract

This article presents a wide conversion ratio bidirectional dc-dc converter based on a bidirectional modified Single-ended primary-inductor converter (SEPIC converter). A key feature of this modified SEPIC converter is the non-dissipative current snubber circuit, which is used to achieve zero current switching and to suppress voltage spikes that occur during MOSFET switching. The snubber is made up of a capacitor, an inductor, and a diode that work together to form a resonant circuit that absorbs the voltage spike and returns it to the circuit without dissipating it. Even with conventional MOSFETs, high efficiency is achieved. The SEPIC converter differs from other bi-directional DC-DC converters in that it provides continuous output current, has fewer components, and can provide high conversion ratios of step-up and step-down voltage without exceedingly low or high duty-cycle. This paper presents a theoretical analysis with stages of operation in both step-up and step-down modes, theoretical waveforms, and the design procedure, as well as a comparison with other bidirectional dc-dc converter topologies.

Key Word: DC-DC Converters; Current Snubber; Power Electronics

1. INTRODUCTION

There is energy extremity all over the world. The increase in demand for energy, global warming and pollution has paved way for the increased dependence on renewable energy sources. The major renewable sources of energy includes sun, wind, geothermal etc., These renewable sources provides sustainable results for the energy extremity. Among the renewable sources, further emphasis is given to Photovoltaic (PV) panels and the Energy Cells (FCs) as they're abundantly available, free from pollution and are sustainable. Still, these renewable sources have the need of storehouse for operation. The store house are used substantially for the purpose of energy buffering where the un-used and redundant energy are stored and released whenever needed. The storehouse bias substantially used is different technology batteries, ultracapacitors and supercapactiors. The block diagram representation of BDC is shown in Fig.1. Through electro-chemical reactions that are reversible the batteries are able to store energy, hence it consumes much extra time for consumption of energy and discharging. The charge-discharge life spans of the batteries are limited. Ultra-capacitors have highly-reversible storage mechanism and because of this it has a very long lifespan. Furthermore, the have very high absorption and discharge rates. An Interfacing circuit is required to connect the input and DC link to be able to give consistent electricity by employing replenishable source of energy. The interfacing circuit has able to step up the voltage when energy is required via use of the storage device and it has able to curtail the voltage whilst charging storehouse device. Hence, for this purpose BDC are utilized. It acts as the interfacing circuit. still, the main shortcoming of these systems are that output voltage taken away the photovoltaic (PV) panels are small and it's inadequate in comparison to rated voltage of the load devices. In order to resolve this issue and satisfy the needed voltage, if numerous batteries are connected in strings in series it would give rise to various issues

such as reduced battery lifetime and reliability issues. To adjust the output voltage to the required level, converters must operate at a high conversion rate. In order to make the BDC compact and light, high switching frequency is used. But, for increased switching frequency there are losses in switches and also increased electromagnetic interference (EMI) is observed. To reduce the switching losses, soft switching is presented.

Many topologies have been drawn in the development of bidirectional dc-dc power converter (BDC). Several approaches are made mainly to meet the drawbacks of traditional buck-boost converter, buck converter and boost converters. Isolated and non-isolated topologies could be utilized for this development. The isolated topologies of the converter design can obtain very high point ratio of conversion via adjusting transformers turns ratio.

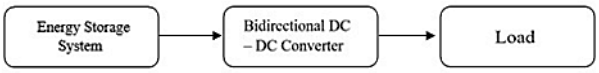

Fig.1. General Block Diagram of BDC

The coupled inductor (CL) method and a voltage tripler rectifier circuit [1] are deployed to reduce switching losses by minimizing the quasi-resonance behavior caused by leakage inductance in the coupled inductors and capacitors circuit. In addition, voltage boosting, switched-inductors, switched-capacitors, voltage lifting techniques (VL) are used to improve the converter's performance. CLBC and SLBC, stacked and cascaded coupled inductor boost converters, and it is used to elevate the voltage gain. A BDC in accordant with the switched-quasi-z-source common ground having extensive range of voltage gain [2] have a large-scale range of gain in voltage, making it ideal for applications such as Electric Vehicles with other Hybrid Energy resources. The device functions with uninterrupted conduction mode, assuming that all power semiconductors and energy storage components are perfect. A group of soft- swtiching BDC [3] are designed to have extended range of zero voltage switching. It is implemented with two supplementary voltage sources, having utilized the passive components, to broaden ZVS operation range. The converter is intended to maintain soft-switching features for the entire operation gamut of duty cycles of the converter, No affixed voltage stress is observed to be exerted on primary switch, while secondary switches experience reduced voltage stress. A new step up SEPIC converter mainly in accordance for replenishable energy applications [4] is developed employing a coupled inductor with a voltage booster cell to attain increase gain of voltage while also recycling the amount of energy contained. It provides stable input current and reduced voltage stress on semiconductors. In comparison to present systems, a BDC that is totally soft-switched [5] and has just one auxiliary switch is intended to reduce system complexity. An approach to decrease the ripple in the commutation torque in the BLDC through the deployment of the modified SEPIC converter and the three-stage NPC Inverter. It involves a amalgamation of a three-level diode which is attached to a multilevel inverter.

2. PROPOSED METHOD

The traditional unidirectional Single Ended Primary Inductor Converter (SEPIC) Converter is used as a buck-boost converter. It has been applied in several applications. Fig.2 represents a traditional unidirectional SEPIC converter. However, the key demerit of the above topology is the restricted static gain and the sum of the output and the input voltages is equal to the voltage stress of the semiconductor. Hence, this structure is modified through the addition of a diode and capacitor. Fig.3. represents modified SEPIC converter. This topology has an increased static gain with one-way operating arrangement. In this construction, the voltage stress across the switches is also reduced. This converter has good efficiency and has been used in panoramic range of applications like replineshable energy systems, motor drive systems and LED driver. For a bidirectional structure, the initial step is to replace the Diodes D1 and D2 in the unidirectional structure with the active switches S_2 and S_3. This bidiriectional structure is shown in Fig.3. The switches S_2-S_3 are used for Buck operation and is operated simultaneously. The switch S_1 is used for Boost operation and is operated complementary to switches S_2-S_3.

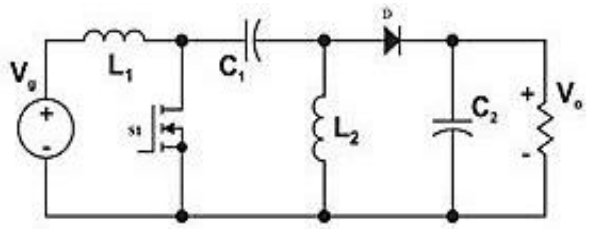

Fig.2. SEPIC Converter

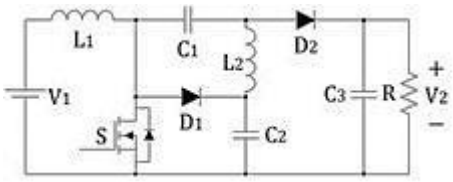

Fig.3. Modified SEPIC Converter

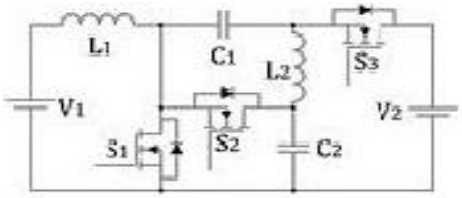

Fig.4. Modified Bidirectional SEPIC Converter

2.1. MODE OF OPERATION

A. OPERATION STAGES WITHOUT CURRENT SNUBBER

The voltage source V_2 is assumed to be higher than the voltage source v_1, and the presented converter has two stages of operation such as the step-up mode and the step-down mode. The operation stages are same in both the modes only with current flow inversion. The theoretical analysis of this dc-dc converter is discussed in the step-up mode, and, there are some rumination in the step-down mode of operation and they are analysed.

1. Operation Stage – FIRST - Step-Up Mode of Operation [Fig.6(a)]: S_1 is activated in this stage, S_2 and S3 are deactivated, and is represented in Fig. 6(a). The two inductors, L_1 and L_2, function as energy storage devices. Specifically, L_1 stores energy with a voltage of V_1 applied across it, while the voltage across L_2 is equal to the voltage difference between node C_2 and node C_1, which is also equal to V_1. Through this configuration, both inductors can effectively store energy.
2. Operation Stage – SECOND - Step Up Mode of Operation [Fig. 6(b)]: S_1 switch is deactivated, and the intrinsic diodes in S_2 and S_3 begins to conduct the current of the inductors. Energy transference is seen from inductors L_1, L_2 to the capacitors in this converter during this stage of operation, that is depicted in Fig.6(b). Voltage that is applied over L_1 and L2 is identical to $(VC_2 - V_1) = (V_1 - VC_2)$ for L_1 and $-(V_2 - VC_2) = (VC_2 - V_2)$ for L_2..

B. OPERATION STAGES WITH CURRENT SNUBBER

(i) STEP-UP MODE OF OPERATION

S_1 switch is commanded, and the S_2 and S_3 switch intrinsic diodes conduct in a reciprocal way to the switch S_1. The stage one of operation is considered when the converter operation is before the S_1 switch conduction command. A delay is given at the command signals of the switches.

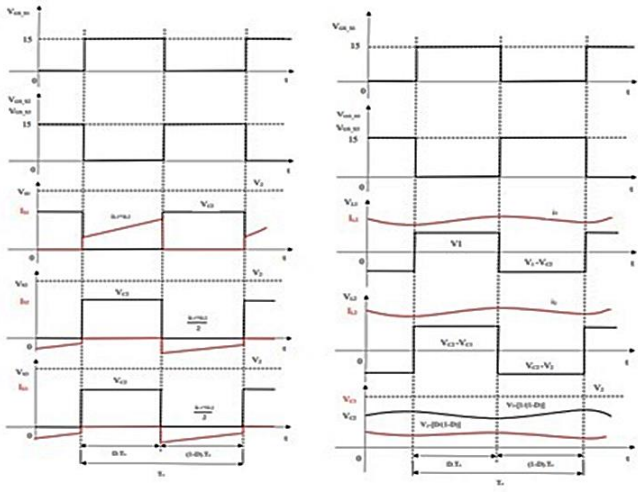

Fig 5 Theoretical Waveforms for Operation of SEPIC Converter

1. *First Stage of Operation:* In this stage energy is transferred from the L_1 and L_2 inductors to the voltage source V_2. This energy transfer is via switch S_3 intrinsic diode. There is decrease of inductor currents linearly. When the switch S_1 turn ON command is processed this stage finishes. This stage of operation is represented in Fig.7.1(a).
2. *Second Stage of Operation:* In this stage the S_1 switch is in ON condition. There is a linear increase in the switch current and decrease in the current of S_3 intrinsic diode. The Snubber inductor L_S limits the di/dt. The voltage that is applied across the L_S inductor is equal to $(V_2 - V_{C1})$. There is storage of energy in both the inductors and the voltage is V1. In this stage, the intrinsic diodes of S_3 switch is null. The diode is also blocked without any reverse recovery current as there is di/dt limitation. This limitation is imposed by the L_S inductor. With this, the second stage of operation ends. This stage of operation is represented in Fig.7.1(b).
3. *Third Stage of Operation:* There is transfer of energy that is stored in the L_s inductor and to C_S via S_1. In this stage, intrinsic diode of S_3 is blocked. Resonant way of energy transfer occurs in this stage of operation. The D_{S2} current diode becomes zero and with this third stage ends. This stage of operation is represented in Fig.7.1(c).
4. *Fourth Stage of Operation:* In this stage conduction of S_1 takes place. The D_{S2} diode remains blocked. The storing of energy continues in this stage in both the inductors. During the turn-on period of S_1, this operation stage is maintained. This stage of operation is represented in Fig.7.1(d).
5. *Fifth Stage of Operation:* In this stage, S_1 switch is turned OFF. There is a linear increase in current and the inductor L_S limits it. The intrinsic diode of S_3 switch conducts at this stage. The energy that is stored in the snubber capacitor C_S during the third stage of operation is discharged in this stage through D_{S1}. This stage comes to an end when, the D_{S1} current becomes zero and the diode is blocked. This stage of operation is represented in Fig.7.1(e).
6. *Sixth Stage of Operation:* In this stage of operation, the switch S_2 intrinsic diode conducts and the D_{S1} diode is blocked. There is linear increase of the current of the intrinsic diode of switch S_3. The S_2 switch intrinsic diode current decreases linearly. The L_1 inductor current becomes equal to the snubber current L_S. There is zero blocking of the S_2 switch intrinsic diode leaving out any reverse recovery current. S_2 switch is closed. There is energy transfer from the inductors L_1 and L_2 to the voltage source V_2 and is returned to the stage one of operation. This stage of operation is represented in Fig.7.1(f).

(ii) STEP-DOWN MODE OF OPERATION

The S_2 and S_3 switches are commanded and there is complementary command to the switch S_1 intrinsic diode. The first stage of operation is considered when the converter operation precedes the S_1 switch conduction command

1. *First Stage of Operation:* This stage is the free-wheeling stage of operation. In this stage, there is transfer of energy from L_1 inductor to the voltage source V_1 and from L_2 inductor to capacitor C_2 via the intrinsic diode of S_1. At the conclusion of this phase, the power switch S_3 is activated. It is represented in Fig.7.2(a).
2. *Second Stage of Operation:* Due to the delay command of the stage, S_2 is deactivated and S_3 is turned ON with Zero Current Switching. There is linear increase of S_3 switch current. There is linear decrease of current of the switch S_1. The inductor L_S limits the decrease of S_1 current. There is also increase of L_1 and L_2 inductors current. When the S_1 intrinsic diode current will become null at the end of this stage. Blocking of S_1 intrinsic diode takes place because of the limitation of di/dt. This limited is imposed by the snubber inductor L_S without any reverse recovery current. This stage of operation is represented in Fig.7.2(b).

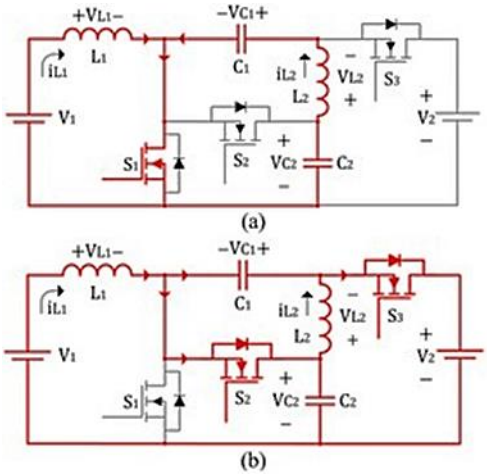

Fig. 6. Stages of Operation

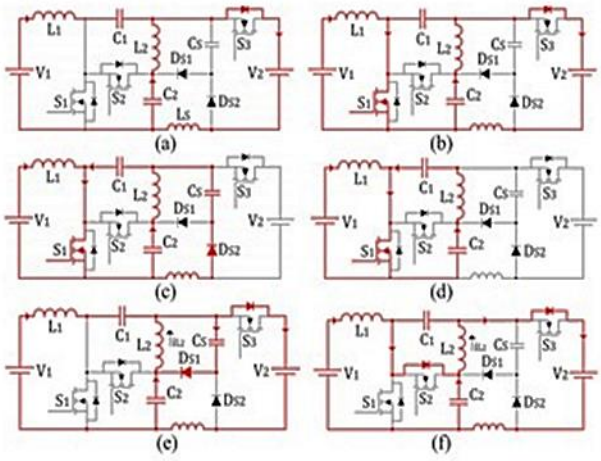

Fig.7.1. Stages of Operation of Step up Mode

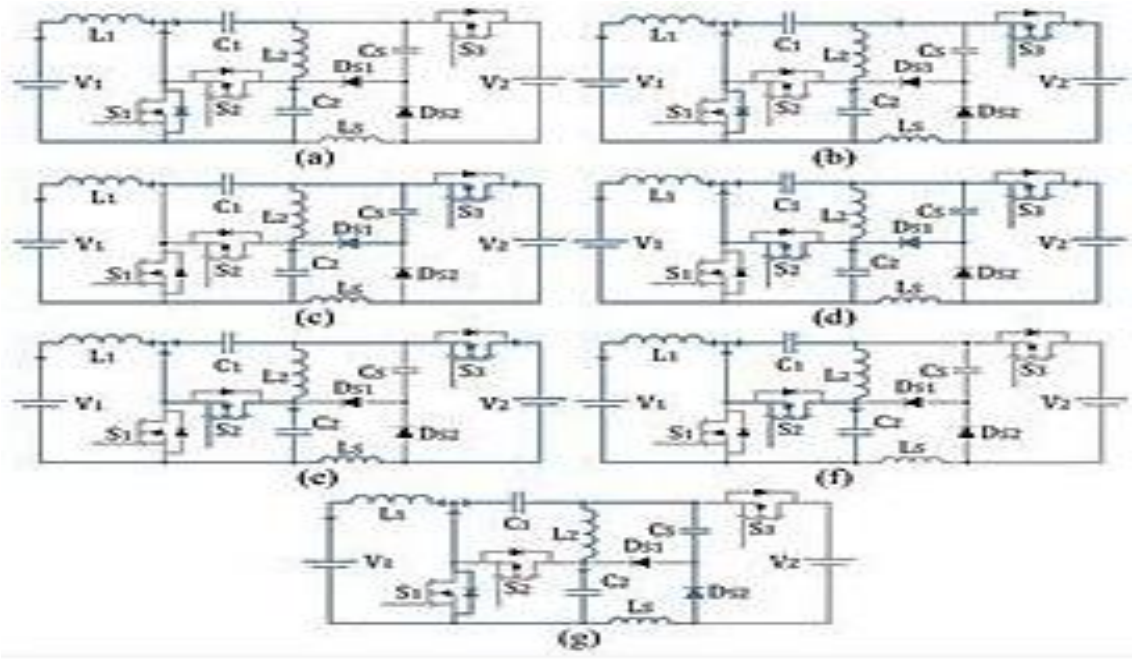

Fig.7.2.Stages of Operation in Step Down Mode

3. *Third Stage of Operation*: In this stage of operation, the intrinsic diode of the switch S_1 is blocked. Both the capacitors C_S and C_2 are charged during this stage of operation. There is transfer of energy from V_2 source via L_S and D_{S1}. There is a linear decrease in the S_3 current and L_S current as well. In this stage, the switch S_2 is turned ON. This stage of operation is represented in Fig.7.2(c).
4. *Fourth Stage of Operation:* Under Zero Current Switching, the switch S_2 is turned ON. There is linear increase of current in this switch. The blocked of diode D_{S1} occurs without any reverse recovery current. Until the diode D_{S1} current becomes zero, the capacitor C_S is charged. This stage of operation is represented in Fig.7.2(d).
5. *Fifth Stage of Operation:* The beginning of this stage is marked by the blocking of D_{S1} diode. The S_2 switch current rises gradually, on the contrary, S_3 switch current decreases linearly. The end of this stage is marked when both the currents of L_S and S_3 are zero. This stage of operation is represented in Fig.7.2(e).
6. *Sixth Stage of Operation:* In this stage of operation, the inductor currents L_1 and L_2 are conducted through the switch S_2. There is transfer of energy to the source V_1. The inductors current increase linearly. There is energy transference and the S_2 switch current also increases linearly. The end of this stage is marked when the S_2 switch and S_3 switch is turned OFF simultaneously. This stage of operation is represented in Fig.7.2(f).
7. *Seventh Stage of Operation:* At this point, S_2 and S_3 are in deactivated condition. The intrinsic diode of S_1 switch conducts. Now, freewheeling stage of both the inductors L_1 and L_2 currents begins. Transference of energy occurs to C_1 via D_{S2} diode and L_S in a resonant way from the C_S capacitor. The D_{S2} diode is blocked when the resonant cycle finishes and it is returned to the first stage of operation. This stage of operation is represented in Fig.7.2(g).

B. DESIGN

The design calculations for the SEPIC Converter are

A. Static Gain

The static gain of the converter is determined by using the energy balance equations. At steady state, in all the inductors in the converter the average voltage is considered to be null. Using the following equations

$$V_{L1\_avg} = V_1 D + (V_1 - V_{C2}).(1 - D) = 0 \quad (1)$$

$$V_{L2\_avg} = (V_{C2} - V_{C1})D + (V_{C2} - V_2)(1 - D) = 0 \quad (2)$$

Through equation 1 the voltage that is applied across C_2 is obtained. The voltage is observed to be equal to the boost converter's static gain. This is represented in equation 3. Across all the semiconductor switches S_1, S_2, S_3 the voltage is equivalent to V_{C2}

$$V_{C2} = \frac{V_1}{1-D} \quad (3)$$

In all inductors in the converter at the steady state the mean voltage is considered to be null as considered above, the relationship between the two capacitors C_1 and C_2 is found to be equal

$$V_{C2} = V_{C1} - V_1 \quad (4)$$

When we substitute the equation 3 in equation 4, the voltage that is across the C_1 capacitor can be obtained using the formula below

$$V_{C1} = \frac{V_1 . D}{1-D} \quad (5)$$

On substituting the equations 3 and 5 in the equation 2, the gain can be computed using below formula

$$\frac{V_2}{V_1} = \frac{1+D}{1-D} \quad (6)$$

B. Inductors Design

The values of L_1, L_2 is calculated over the function of the current ripple ($\Delta i_{L1} - \Delta i_{L2}$). The voltage that is applied across the inductors when there is turn on of switch S_1 will be equal to the voltage V_1. It is represented in equation 7 and 8. The mean currents of the L_1, L_2 are obtained to be identical to the mean currents of V_1 and V_2

$$L_1 = \frac{V_1.D}{\Delta_{iL1}.f_s} \quad (7)$$

$$L_2 = \frac{V_1.D}{\Delta_{iL2}.f_s} \quad (8)$$

C. Capacitors Design

The values of the capacitors C_1 and C_2 are calculated using the variation of charge and also the specifications of the voltage ripple such as ($\Delta V_{C1} - \Delta V_{C2}$). The equations 9 and 10 the value of the capacitor values C_1 and C_2 can be calculated. During the stage 1 of operation, the current that is across the capacitors C_1 and C_2 will be equal to the current of L_2 inductor. The average value is observed to be equivalent to the mean current of V_2 (i_{V2}).

$$C_1 = \frac{iV_2.D}{\Delta_{VC1}.f_s} \quad (9)$$

$$C_2 = \frac{iV_2.D}{\Delta_{VC2}.f_s} \quad (10)$$

D. Design of Snubber

In this article, the converter that is proposed is designed with the current snubber circuit inclusion that is non-dissipative. The main purpose of the active or passive snubber circuit method is that it provides lossless switching for the semiconductor active power switches in both of the direction of power flows. Here non-dissipative snubber circuit is developed using only passive components. It reduces switching losses and it also allow the usage of conventional Si MOSFETs. The snubber circuit consists of a capacitor C_s, resonant inductor L_s, and diodes, D_{S1} and D_{S2}. The snubber circuit operates with zero current switching commutation at the working stage of switches and in deactivated stage of some switches. This snubber is used to limit the *di/dt*. In the intrinsic diodes in the switches, the reverse recovery current is also limited.

$$L_S = \frac{\alpha(V_1+V_{C2})}{(L_{L1}+I_{L2})} \quad (11)$$

Value of Ls could be determined by setting a minimum delay time (α) which is greater to the duration of interval t_2 depicted in the suppositional waveforms during step-down operation. The snubber Ls could be brought using formula that takes into account the specified time delay. Using the L_S inductor specification, one can compute the value of the snubber capacitor C_S. This calculation involves the determination of the period of resonant (T_o) of resonant energy transfer equation, which can be obtained through the given formula :

$$\frac{T_0}{2} = \pi.\sqrt{L_S.C_S} \quad (12)$$

Equation 13 shows the maximal voltage that is applied in through the D_s . From the waveforms it can be observed that the period of conduction of them is diminished and the median current is reduced in these diodes. The specification of them is dependent on the high peak current of the circuit.

$$V_{DS1} = V_{DS2} = V_{C2} = \frac{V_1}{1-D} \quad (13)$$

The specifications of converter is shown in Table 1

Parameter	Value
L_1	270 μH
L_2	3.18 *mH*

L_S	10 µH
C_1-C_2	4.8 µF
C_S	1 µF
S_1-S_2-S_3	IRFP4868
D_{S1}-D_{S2}	MUR1560

3. RESULTS

The simulation diagram, the hardware prototype and the results are presented below.

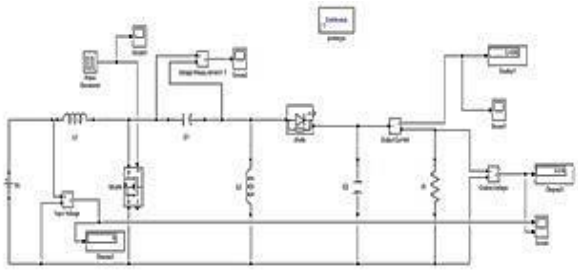

Fig.9. Simulation of SEPIC Converter

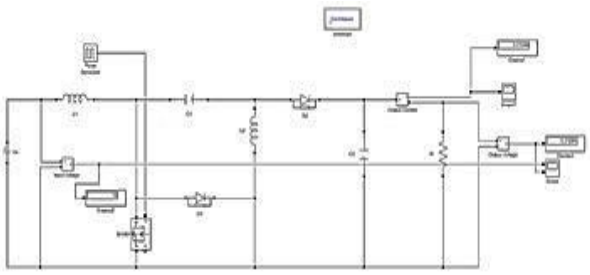

Fig.10. Development of Modified SEPIC Converter

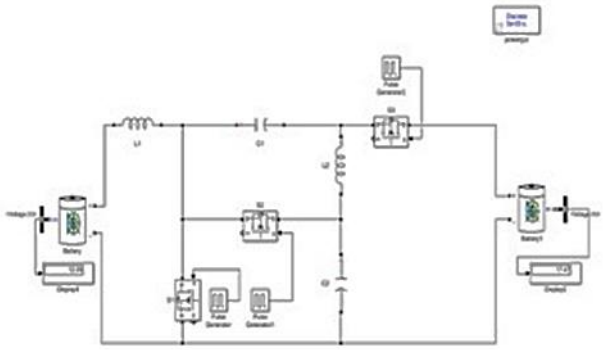

Fig.11. Development of modified SEPIC converter

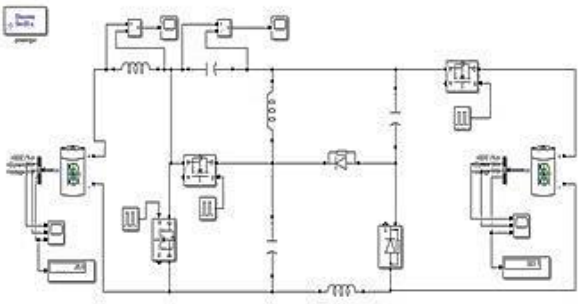

Fig.12. Open loop configuration of BDC

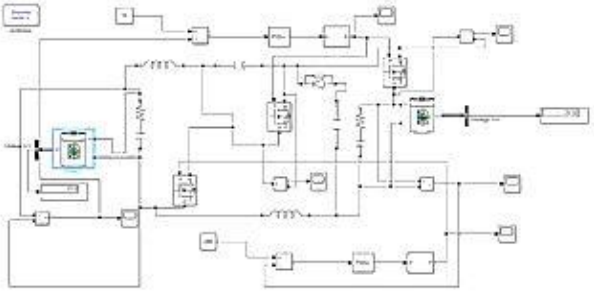

Fig.13. Closed loop configuration of BDC

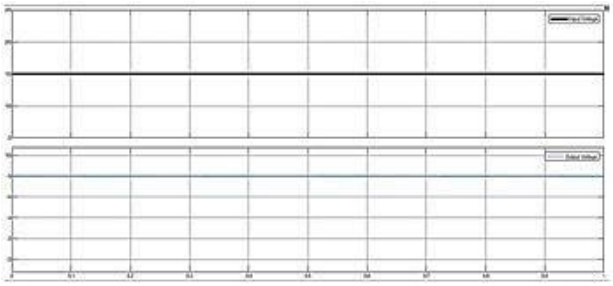

Fig.14. Input and Output waveform – Buck Mode Mode

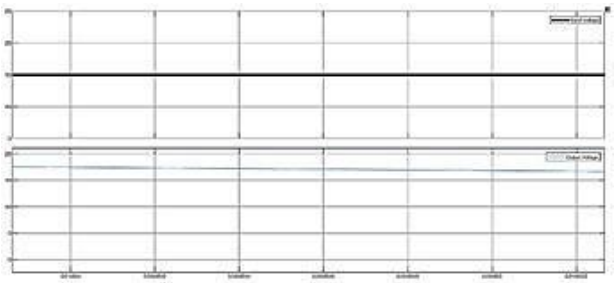

Fig.15. Input and Output waveform – Boost

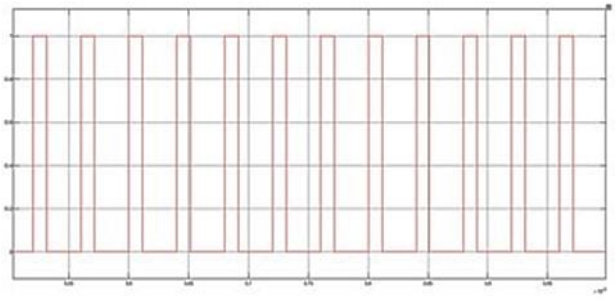

Fig.16. Input pulse waveform

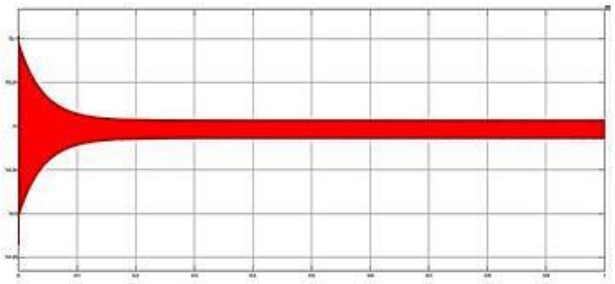

Fig.17. C_s Volatge Waveform

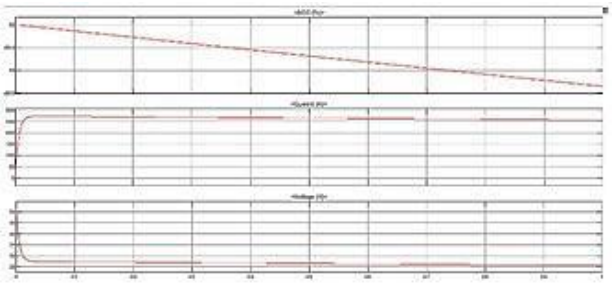

Fig.18. Battery Waveform

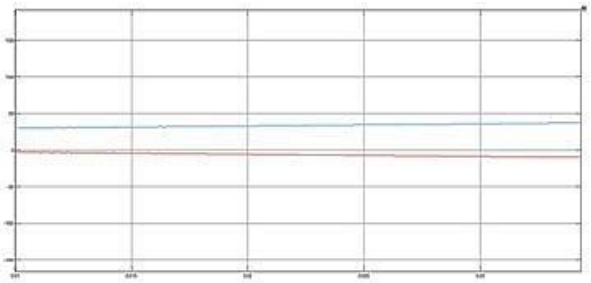

Fig.19. Voltages of Capacitor C_1 and C_2

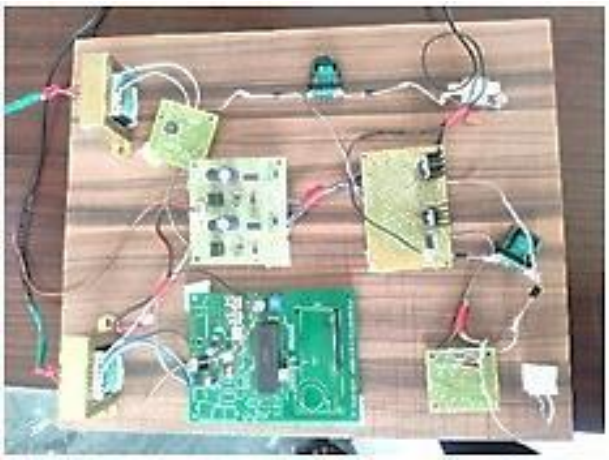

Fig.20. Experimental Hardware setup

Fig.21. Voltage output in Boost and Buck mode

Fig.22. Voltage across Inductor L_s

4. CONCLUSION

In this paper, a bidirectional converter based on modified SEPIC converter has increased conversion ratio is presented. This allows reduced number of switches and obtains good conversion in both buck and boost mode. The proposed converter has an supplementary non-dissipative current snubber, and this provides soft switching of the active semiconductor power switches and this eliminates the issue of reverse recovery in the intrinsic diodes of semiconductor power switches. This minimizes the voltage stress that is on the power switches. It utilizes reduced count of components and obtains high voltage in the boost mode of operation.

REFERENCES

1. S. Hasanpour, A. Baghramian, and H. Mojallali, "A modified SEPIC based high step-up DC–DC converter with quasi-resonant operation for renewable energy applications," IEEE Trans. Ind. Electron., vol. 66, no. 5, pp. 3539–3549, May 2019, doi: 10.1109/tie.2018.2851952.
2. Y. Zhang, Q. Liu, J. Li, and M. Sumner, "A common ground switched quasi-Z-source bidirectional DC–DC converter with wide-voltage-gain range for EVs with hybrid energy sources," IEEE Trans. Ind. Electron., vol. 65, no. 6, pp. 5188–5200, Jun. 2018, doi: 10.1109/tie.2017.2756603.
3. M. R. Mohammadi and H. Farzanehfard, "Family of soft-switching bidirectional converters with extended ZVS range," IEEE Trans. Ind. Electron., vol. 64, no. 9, pp. 7000–7008, Sep. 2017, doi: 10.1109/ tie.2017.2686308M.
4. Y. Wang, S. Gao, and D. Xu, "A 1-MHz-modified SEPIC with ZVS characteristic and low-voltage stress," IEEE Trans. Ind. Electron., vol. 66, no. 5, pp. 3422–3426, May 2019, doi: 10.1109/tie.2018.2851974
5. R. Moradpour, A. Tavakoli, and H. Ardi, "Design and implementation of a new SEPIC-based high step-up DC/DC converter for renewable energy applications," IEEE Trans. Ind. Electron., vol. 65, no. 2, pp. 1290–1297, Feb. 2018, doi: 10.1109/TIE.2017.2733421.
6. S. Rahimi, M. Rezvanyvardom, and A. Mirzaei, "A fully soft-switched bidirectional DC–DC converter with only one auxiliary switch," IEEE Trans. Ind. Electron., vol. 66, no. 8, pp. 5939–5947, Aug. 2019, doi: 10.1109/tie.2018.2873535.
7. V. Viswanathan and J. Seenithangom, "Commutation torque ripple reduction in the BLDC motor using modified SEPIC and threelevel NPC inverter," IEEE Trans. Power Electron., vol. 33, no. 1, pp. 535–546, Jan. 2018, doi: 10.1109/tpel.2017.2671400
8. H. Wu, K. Sun, L. Chen, L. Zhu, and Y. Xing, "High step-up/step-down soft-switching bidirectional DC–DC converter with coupled-inductor and voltage matching control for energy storage systems," IEEE Trans. Ind. Electron., vol. 63, no. 5, pp. 2892–2903, May 2016, doi: 10. 1109/TIE.2016.2517063.
9. N. Molavi, E. Adib, and H. Farzanehfard, "Soft-switching bidirectional DC–DC converter with high voltage conversion ratio," IET Power Electron., vol. 11, no. 1, pp. 33–42, Jan. 2018, doi: 10.1049/ietpel.2016.0771.

10. M. Kwon, S. Oh, and S. Choi, "High gain soft-switching bidirectional DC–DC converter for eco-friendly vehicles," IEEE Trans. Power Electron., vol. 29, no. 4, pp. 1659–1666, Apr. 2014, doi: 10.1109/ tpel.2013.2271328.
11. D. R. Patil, A. K. Rathore, and D. Srinivasan, "Non-isolated bidirectional soft-switching current-fed LCL resonant DC/DC converter to interface energy storage in DC microgrid," IEEE Trans. Ind. Appl., vol. 52, no. 2, pp. 1711–1722, Mar./Apr. 2016, doi: 10.1109/TIA.2015.2498127.
12. C.-M. Lai, Y.-C. Lin, and D. Lee, "Study and implementation of a two phase interleaved bidirectional DC/DC converter for vehicle and DC microgrid systems," Energies, vol. 8, no. 9, pp. 9969–9991, Sep. 2015, doi: 10.3390/en8099969.
13. H. Ardi, A. Ajami, F. Kardan, and S. N. Avilagh, "Analysis and implementation of a nonisolated bidirectional DC–DC converter with high voltage gain," IEEE Trans. Ind. Electron., vol. 63, no. 8, pp. 4878–4888, Aug. 2016, doi: 10.1109/TIE.2016.2552139.
14. L.-S. Yang and T.-J. Liang, "Analysis and implementation of a novel bidirectional DC–DC converter," IEEE Trans. Ind. Electron., vol. 59, no. 1, pp. 422–434, Jan. 2012, doi: 10.1109/TIE.2011.2134060.
15. P. De Melo, R. Gules, E. Romaneli, and R. Annunziato, "A modified SEPIC converter for high-power-factor rectifier and universal input voltage applications," IEEE Trans. Power Electron., vol. 25, no. 2, pp. 310–321, Feb. 2010, doi: 10.1109/tpel.2009.2027323.
16. R. Gules, W. M. Dos Santos, F. A. Dos Reis, E. F. R. Romaneli, and A. A. Badin, "A modified SEPIC converter with high static gain for renewable applications," IEEE Trans. Power Electron., vol. 29, no. 11, pp. 5860–5871, Nov. 2014, doi: 10.1109/tpel.2013.2296053.
17. Y. T. Yau, W. Z. Jiang, and K. I. Hwu, "Bidirectional operation of high step-down converter," IEEE Trans. Power Electron., vol. 30, no. 12, pp. 6829–6844, Dec. 2015, doi: 10.1109/TPEL.2015.2392376.
18. J. De Matos, F. E Silva, and L. Ribeiro, "Power control in AC isolated microgrids with renewable energy sources and energy storage systems," IEEE Trans. Ind. Electron., vol. 62, no. 6, pp. 3490–3498, Jun. 2015, doi: 10.1109/tie.2014.2367463.
19. P. Shreelakshmi, M. Das, and V. Agarwal, "Design and development of a novel high voltage gain, high-efficiency bidirectional DC–DC converter for storage interface," IEEE Trans. Ind. Electron., vol. 66, no. 6, pp. 4490–4501, Jun. 2019, doi: 10.1109/tie.2018.2860539.
20. R.-J. Wai, R.-Y. Duan, and K.-H. Jheng, "High-efficiency bidirectional dc–dc converter with high-voltage gain," IET Power Electron., vol. 5, no. 2, pp. 173–184, 2012, doi: 10.1049/IET-PEL.2011.0194.
a. A. Fardoun, E. H. Ismail, A. J. Sabzali, and M. A. Al-Saffar, "Bi-directional converter with low input/output current ripple for renewable energy applications," in Proc. IEEE Energy Convers. Congr. Expo., Sep. 2011, doi: 10.1109/ecce.2011.6064217.
21. Y.Zhang, Y. Gao, L. Zhou, and M. Sumner, "A switched-capacitor bidirectional DC–DC converter with wide voltage gain range for electric vehicles with hybrid energy sources," IEEE Trans. Power Electron., vol. 33, no. 11, pp. 9459–9469, Nov. 2018, doi: 10.1109/ TPEL.2017.2788436.